-Technical Paper-

CYCLIC LOADING TESTS ON SOFT-FIRST-STORY RC FRAMES RETROFITTED WITH THICK HYBRID WING-WALL

Pasha JAVADI*[1], Tetsuo YAMAKAWA*[2], Makoto KOBAYASHI*[3], Michiyo GAJA*[4]

ABSTRACT

Three one-bay two-story RC frames which had the characteristics of soft-first-story frames (pilotis frames) were retrofitted with thick hybrid wing-wall method to find out a desired seismic performance and consequently propose an appropriate scheme of this retrofit type. In retrofitting procedure, channel-shaped steel plates jacketed the boundary columns of the soft-story and extended to the bay of the frame through the additional steel plates. In this method, the additional thick hybrid wing-walls not only increase the lateral strength and stiffness of RC frames, but also considerably improve the ductility of non-ductile RC frames.

Keywords: soft-first-story, pilotis frame, seismic retrofitting, seismic strengthening, thick hybrid wall

1. INTRODUCTION

Numerous total and partial collapses of reinforced concrete (RC) buildings occurred during the 1995 Kobe earthquake in Japan. Soft-first-story (i.e., pilotis) mechanism was the most common type of failures that occurred due to discontinuity of lateral resisting system in the ground floor to provide retail occupancy or parking. Nowadays, a large number of reinforced concrete buildings in use have similar characteristics to those that collapsed during the past earthquakes.

Previous investigations by Rahman et al. [1] on one-bay one-story RC bare frames demonstrated that utilizing thick-hybrid-wall method not only significantly increases the lateral strength and stiffness of soft-story frames, but also considerably improves the ductility of the retrofitted frame, and therefore the proposed technique provided an adequate seismic performance.

In this paper, the attention mainly focuses on obtaining a desirable retrofit scheme of thick hybrid wing-wall for soft-first-story RC frames. Three one-bay two-story specimens with soft-first-story characteristics were planed to retrofit with different schemes to verify the possible failures modes of this retrofit type.

2. TEST PLAN

In this study, experimental investigations were conducted on three soft-first-story frames retrofitted by thick hybrid wing-wall method. In all of the test specimens, the geometric dimensions and the reinforcement patterns of the RC frames were identical. Dimensions of sections, reinforcements details and properties of materials are given in Fig. 1 and Table 1, respectively. All specimens were fabricated in two stages. In the first stage, the RC frames were cast and cured, and in the second stage, after 28 days, the additional concrete of the wing-walls were cast (see Fig. 2). Main objective of design of test specimens with different retrofitting details is to find out a desired retrofit scheme.

The specimens were subjected to constant axial loads ($N=0.2\sigma_B bD$ per column) by force-controlled program and to cyclic horizontal loads by displacement-controlled program. In order to provide the lateral distribution of seismic induced force in the height of building, at each horizontal loading stage, 5/11 and 6/11 of the base shear force were applied on the first and second stories, respectively, according to the factor (Ai) for vertical distribution of the seismic story shear force used in Building Standard Law of Japan. The displacement-controlled program and the schematic view of test setup are illustrated in Fig. 3.

As shown in Fig. 2, specimen **R07P-P0** is a soft-first-story benchmark specimen. The shear span-to-depth ratio of the columns (considering their clear heights) is M/Vd=2.5, and that of the top beam (considering its clear span) is M/Vd=2.65. The scale factor of test specimens was about 1/4~1/3 of a low-rise school building designed to the pre-1971 Building Standard Law of Japan. The ratio of transverse reinforcement of the column was the poor amount of ρ_w=0.12%, and the ratio of their longitudinal reinforcements was ρ_g=1.85%. The lateral strength and stiffness of the second story which consisted of shear wall was considerably greater than first story to obtain a frame with soft-first-story behavior.

Specimen **R06P-WW** was retrofitted with thick

*1 Graduate Student, Graduate School of Eng. and Science, University of the Ryukyus, M. Eng., JCI Member
*2 Prof., Department of Civil Eng. and Architecture, University of the Ryukyus, Dr. Eng., JCI Member
*3 Graduate Student, Graduate School of Eng. and Science, University of the Ryukyus, JCI Member
*4 Research Assistant, University of the Ryukyus, JCI Member

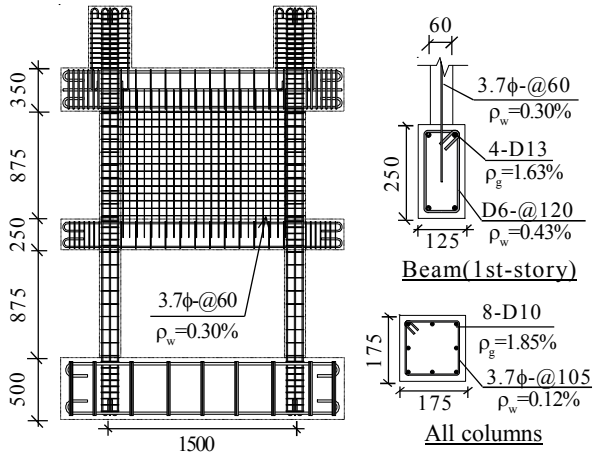

Fig. 1 Details of reinforcements (unit: mm)

hybrid wing-wall. In retrofitting procedure, channel-shaped plain steel plates (t=2.3mm) jacketed the boundary columns, and extended into the bay of the first story through the additional deck steel plates (t=1.2mm). Bolts (M12) were stitched the deck steel plates installed at two sides of the column. In this case-study, the depth of the additional wing-wall (2D) was two times of the depth of the column (D), and its width was equal to that of the column. To prevent crushing of concrete at the exposed face of wing-wall, transverse reinforcements (D6-@100mm) were arranged at the exterior side of the wing-wall. The steel plates were also used as a formwork for casting the additional concrete of wing-wall. Additional concrete of wing-wall was cast vertically up to the bottom face of the top beam. After casting the additional concrete, the existing gap (about 10mm) between the exterior faces of the column and steel plates were filled by mortar-grout.

The retrofitting procedure of specimen **R08P-WN** was same as specimen R06-WW, but in this test specimen plain steel plates (t=2.3mm) was used instead of deck steel plates. Also, PC bars (high-strength steel bars, 13ϕ) were stitched the plain steel plates at two sides of the column instead of bolts (M12). After hardening the additional concrete and before test, the PC bars crossing the body of wing-wall were fastened up to a tensile strain of about 2500μ.

In specimen **R08P-WA**, the retrofitting scheme followed same procedure with specimen R08P-WN, but in this specimen it was planed to perfectly prevent the possible shear sliding at the bottom and the top of the additional wing-walls. For the sake of aforementioned reason, the steel plates in the wing-wall parts were extended up to about the middle of the top beam, and they were anchored to the beam by means of PC bars. Moreover, a disk-anchor (see Fig. 4) was installed at the bottom of each wing-wall to suppress the possible shear-sliding at this surface. Disk distributes the shear stress at

Table 1 Properties of steel materials

Steel material		a (cm²)	σ_y (MPa)	ε_y (%)	E_s (GPa)
Rebar or Dowel	D10	0.71	349 [1)]	0.17	202
			355 [2),3)]	0.18	201
	D13	1.27	359 [3)]	0.20	179
			342 [1)]	0.17	201
	M16	1.57	725 [3)]	-	-
Hoop or Stirrup	3.7ϕ	0.11	650 [1)]	0.31	208
			683 [2)]	0.34	202
			617 [3)]	0.33	188
	D6	0.32	432 [1)]	0.25	175
			504 [2)]	0.26	194
			449 [3)]	0.29	153
PC bar	13ϕ	1.33	1220 [2),3)]	0.61	200
Deck plate	t=1.2mm	-	268 [1)]	0.13	203
Plain plate	t=2.3mm	-	348 [1)]	0.16	212
			335 [2)]	0.16	209
			358 [3)]	0.16	218

Notes: a=cross sectional area; σ_y=yield strength of steel; ε_y=yield strain of steel; E_s=Young's modulus of elasticity; [1)] for R06P; [2)] for R07P; [3)] for R08P.

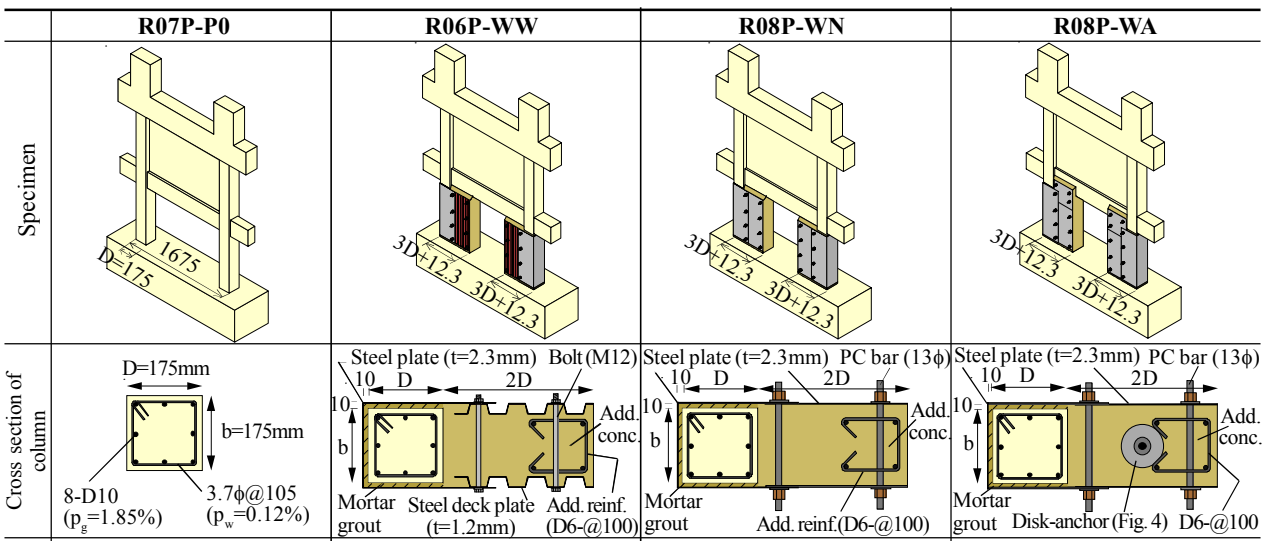

Fig. 2 Details of test specimens

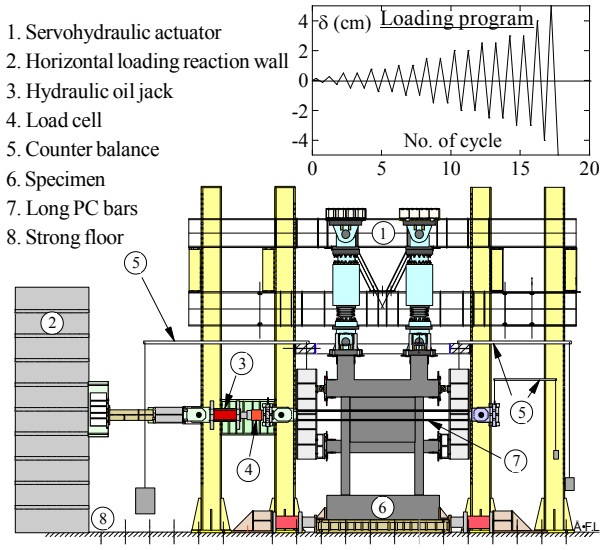

Fig. 3 Test setup and loading program

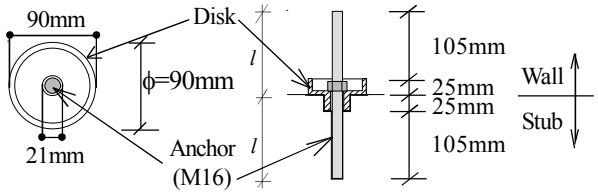

Fig. 4 Details of disk-anchor

the shear sliding plane along its width to suppress the concentration of shear-sliding force induced at potential sliding surface. Anchors were embedded to panel-wall with a length of l=130mm, and to the stub with a length of l=130mm according to manufacturer's instructions. In this specimen, PC bars crossing the body of wing-wall were fastened up to a tensile strain of about 2500μ.

3. EXPERIMENTAL RESULTS AND DISCUSSIONS

In specimen **R07P-P0**, flexural cracks formed at the ends of the columns at drift angle of R=0.5% ($R=\delta/h$, where δ= horizontal displacement of first story and h=the height of first story) as well as shear cracks appeared at the same zones at drift angle of R=0.75%. The lateral strength of the specimen was governed by formation of flexural plastic hinges at both ends of the first story columns, but the specimen finally collapsed due to shear failure at flexural plastic hinge zone in right-side column at drift angle of R=1.64%.

The specimen **R06P-WW** is retrofitted by additional wing-wall. The wing-wall resisted against the lateral load by action of compression strut. Because of long-length arm between tension and compression zones at both ends of wing-wall-column, the longitudinal reinforcements prematurely yielded at drift angle of R=0.3%. After loading test, the jacketing deck steel plates were detached, and it was observed that a diagonal shear crack had formed in each wing-wall. The lateral displacement of the specimen was governed by flexural deformation of wing-wall-column and overall flexural behavior of the specimen (overturning resistance). Considering this combined mechanism, when the specimen was pushed from left to right, it is expected the compression force in the wing-wall at right-side column would be significantly greater than that at left-side column due to overturning resistance. This mechanism was confirmed through the direction of diagonal shear cracks in the wing-walls. In each direction, the wing-wall with higher compression force in its strut diagonally cracked. Calculation of shear strength of wing-

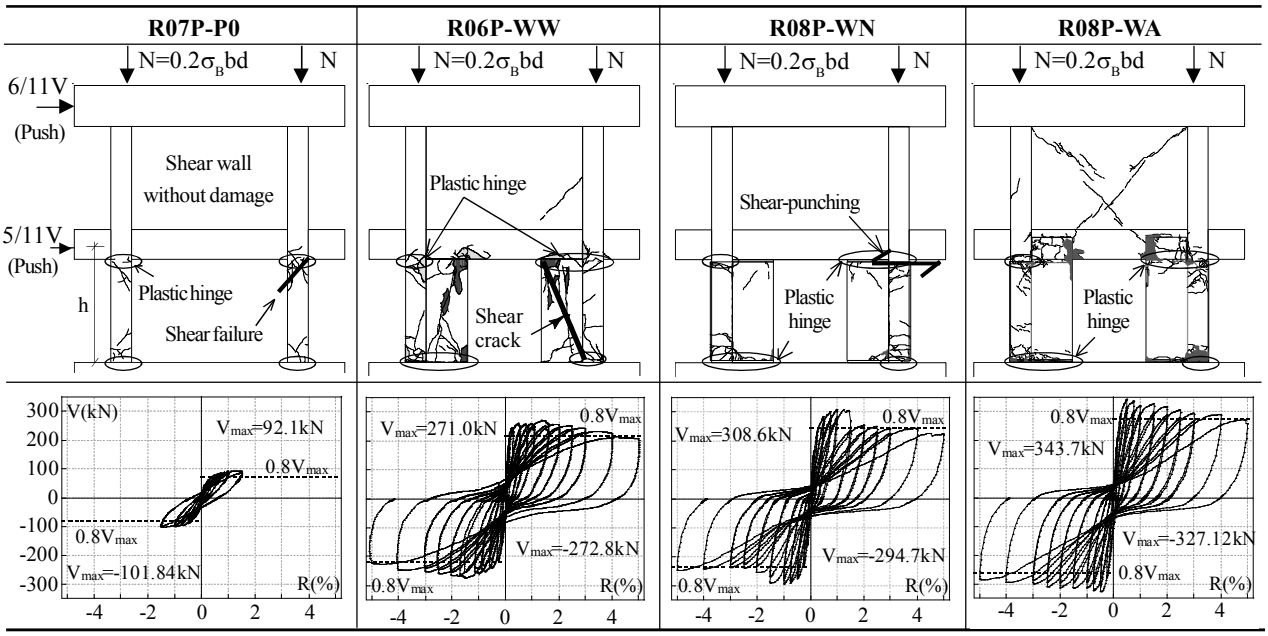

Note: Major mechanisms of the specimens are as follows (due to push loading):
R07P-P0: At first, flexural plastic hinges formed at both ends of the columns, and finally shear failure occurred at the plastic hinge zone of right-side column.
R06P-WW: At left-side column, plastic hinges formed, but at right-side column before perfect formation of plastic hinge, strut of wing-wall cracked.
R08P-WN: Initially the plastic hinge formed at both ends of columns, but as the longitudinal reinforcements at top yielded the punching failure happened.
R08P-WA: Plastic hinges formed at both ends of columns. This mechanism represents the desired performance of this type retrofit.

Fig. 5 Experimental V-R relationships, crack patterns and experimentally observed mechanisms

wall is deferred to Section 4. The governing mechanisms of the specimens are shown in Fig. 5.

In specimen **R08P-WN**, due to long-length arm between tension and compression zones at wing-wall-columns, the longitudinal reinforcements of the boundary columns at bottoms yielded at drift angle of R=0.3%. The flexural cracks appeared at the bottom of the columns at drift angle of R=0.5%. At the top sections of the columns, the flexural tension and compression stresses, and shear-friction stress mainly acted. Since the tension actions of longitudinal reinforcements contribute in both flexural and shear-friction resistances, the exact evaluation of shear-punching at the top of columns becomes complex. In this specimen the sections of columns initially withstood against shear-punching through the shear-friction resistance, but by preceding the loading test, the longitudinal reinforcements gradually entered to the inelastic state due to flexural behavior, and consequently the shear-punching resistance considerably decreased. As the longitudinal reinforcements at the top of column yielded, the lateral resistance of the specimen suddenly dropped due to shear-punching failure (see *V-R* relationship of specimen R08P-WN in Fig. 5). After that, the shear-sliding resistance at the compression zone maintained the lateral strength, and the *V-R* response exhibit a ductile response up to drift angle of R=5.0%.

In specimen **R08P-WA**, the longitudinal reinforcements of boundary columns at bottom yielded at drift angle of R=0.3%. The flexural cracks at the bottom of wing-wall-columns appeared at drift angle of R=0.5%. Moderate strength degradation was obvious in the *V-R* relationship of specimen R08P-WA that results from crushing of concrete at compression zone and buckling of longitudinal reinforcements. The resisting force maintained greater than 0.8 Vmax up to drift angle of R=5.0%, and the overall response of the specimen shows a ductile behavior. To verify the shear sliding resistance carried by steel plates at top of wing-wall, shear strain-gauges were attached at that level. The produced shear force in the steel plates that resisted against shear-sliding

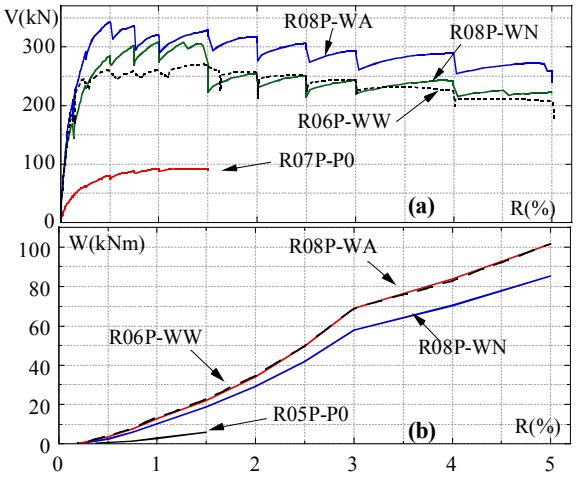

Fig. 6 Comparison of (a) skeleton curve and (b) accumulative absorbed energy

was about 27% of overall lateral strength of the specimen. It should be emphasized the reduction of lateral strength in specimen R08P-WN due to shear-punching failure was about 18% of its overall lateral strength. Comparison between the behavior of specimens R08P-WN and R08P-WA exhibits the efficiency of steel plates in shear-sliding resistance at the top of wing-wall-column. The comparisons of experimental skeleton curves and accumulative absorbed energy are shown in Fig. 6. It should be noted the lateral resisting force of specimen R08P-WA is larger than R06P-WW, but the accumulative absorbed energy is almost same due to different shape of hysteretic response resulting from different mechanisms.

4. CALCULATION OF LATERAL STRENGTHS

The lateral strengths of the specimens were governed by ultimate flexural strength of wing-wall-column, shear sliding at top and bottom of wing-wall-column or the shear resistance of wing-wall-column. The flexural strength of the wing-wall-column can be calculated by section analysis considering two conditions, when the column is in compression or when the wing-wall is in compression. Simplified equations in calculating the flexural strength of wing-wall-column were proposed by Rahman et al. [1]. In this paper, the attention mainly focuses on calculating the shear strength and shear sliding resistance of column retrofitted by thick hybrid wing-wall.

4.1 Shear Strength

In calculating the shear strength of wing-wall-column, both the arch action of wing-wall-column and the shear resistance of jacketing steel plates should be superimposed. The resultant shear strength can be calculated as follows;

$$V = V_a(\text{arch action}) + V_s(\text{steel plate}) \quad (1)$$

(a) Arch Action of Wing-wall-column (V_a)

As shown in Fig. 7, arch action of wing-wall column is calculated based on the proposed approach by Nielsen [2] for a beam without transverse reinforcements. Considering the lower bound solution, the arch can obtain the maximum possible load when the depth of the arch is half of depth of the section. In the proposed mechanism for wing-wall-column, it is considered the depth of the arch is half of depth of the wing-wall-column. The approach to calculate the shear strength is as follows;

$$V_a = 0.5(1+\beta)bD\nu\sigma_B\tan\theta \quad (2)$$

$$\tan\theta = \sqrt{1+\left(\frac{H}{(1+\beta)D}\right)^2} - \frac{H}{(1+\beta)D} \quad (3)$$

$$\nu = 0.7 - \frac{\sigma_B}{200} \quad \text{(for steel deck plate)} \quad (4)$$

$$\nu = 1.0 \quad \text{(for steel plain plate)} \quad (5)$$

where ν is confinement effectiveness factor, σ_B is the cylinder strength of concrete and b is the minimum width

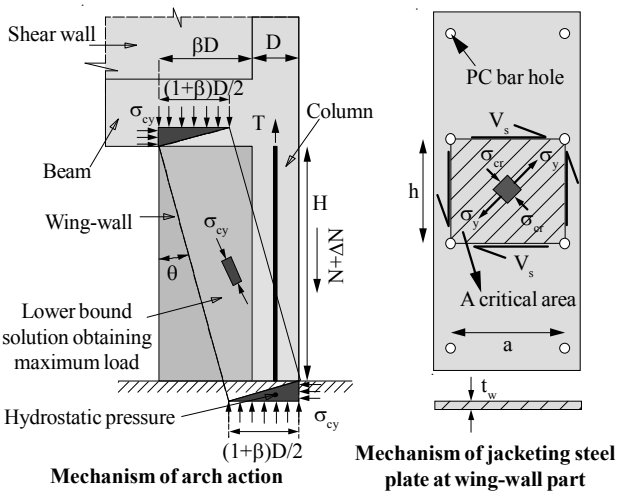

Fig. 7 Shear resistance mechanism

of wing-wall or top beam and other parameters are given in Fig. 7. In case of using steel deck plate, the confinement effect of steel deck plate is neglected due to its low out-of-plane resistance (see Eq. 4). But, in case of steel plain plate, since it has considerable resistance toward out-of-plane deformation, the confinement effect can be considered through the Eq. 5.

(b) Shear Resistance by Steel Plate (V_s)

Since the steel plates are perfectly stitched to additional concrete by means of PC bars, it is expected the steel plate resists in shear. Moreover, there is no bond resistance between the steel plate and concrete, so the produced shear stress at steel plate can not influence the stress on the arch action, such as that happens in truss mechanism for ordinary column due to the bond resistance. Considering this fact, the shear mechanism of steel plate and arch action by concrete can be accounted as two uncoupled mechanism that can be superimposed. The ultimate shear resistance of a critical area can be calculated based on the procedure adapted in AISC-1999 for steel plate girder as reported by Astaneh-Asl [3];

A. For compact steel plate when $h/t_w \le 1.10\sqrt{k_v E/F_{ys}}$:

$$V_s = 0.6 A_w F_{ys} \tag{6}$$

B. For non-compact and slender steel plate when $h/t_w > 1.10\sqrt{k_v E/F_{ys}}$:

$$V_s = 0.6 A_w F_{ys} \frac{1-C_v}{1.15\sqrt{1+(a/h)^2}} \tag{7}$$

$$k_v = 5 + \frac{5}{(a/h)^2} \tag{8}$$

The value of k_v should be taken as 5.0 if a/h is greater than 3.0 or $[260/(h/t_w)]^2$. Value of C_v is given as follows:

(a) if $1.10\sqrt{\frac{k_v E}{F_{ys}}} \le \frac{h}{t_w} \le 1.37\sqrt{\frac{k_v E}{F_{ys}}}$ then $C_v = \frac{1.10\sqrt{k_v E/F_{ys}}}{h/t_w}$

(b) if $\frac{h}{t_w} > 1.37\sqrt{\frac{k_v E}{F_{ys}}}$ then $C_v = \frac{1.51 k_v E}{(h/t_w)^2 F_{ys}}$

where E and F_{ys} are elasticity modulus and yield stress of steel plate. Other parameters are depicted in Fig. 7. In calculating the shear resistance of jacketing steel plate, it was supposed that the shear force perfectly transfer from PC bars to the jacketing steel plate. The shear resistance of PC bars and bearing capacity of the provided holes at steel plates were suggested by Yamakawa et al. [4]. In the most cases, the shear strength of steel plate is the lowest value compared to shear strength of PC bars and bearing capacity of the provided holes.

4.2 Shear Sliding

In column retrofitted by thick hybrid wing-wall, shear sliding is likely to happen at top and bottom of wing-wall-column. The concrete at compression zone and the longitudinal reinforcements withstand against shear sliding by shear friction resistance and dowel action, respectively. If the steel plate at wing-wall part anchored to the beam (such as specimen R08P-WA), the shear sliding resistance at potential sliding plane, at top of wing-wall-column, will considerably increase. Moreover, at the bottom of wing-wall, additional stud dowels or disk-anchors can be installed to ensure the shear sliding resistance. Shear sliding can be calculated by superposition of different components as follows;

1) Total shear sliding resistance:

$$V_n = V_{ns} + V_{nc} + (V_s \text{ or } V_{da}) \tag{9}$$

2) Dowel action resistance by kinking (V_{ns}; for longitudinal reinforcement) [1]:

$$V_{ns} = 0.25 f_y A_s \tag{10}$$

3) Concrete in net compression zone (V_{nc}):

A. For concrete placed against hardened concrete not intentionally roughened [5], when the compression zone is in wing-wall (μ=0.6), see Fig. 7:

$$V_{nc} = \mu N_c < \{0.2\sigma_B A_c \;\&\; 5.5 A_c\};\ (\text{N, mm}) \tag{11}$$

B. For concrete monolithically cast [6], when compression zone is in column (μ=1.4), see Fig. 7:

$$V_{nc} = \mu(\rho_s f_y + N_c) < \{0.2\sigma_B A_c \;\&\; 5.5 A_c\}; \tag{12}$$

$$V_{nc} = \mu N_c < \{0.6\sigma_B A_c \;\&\; 14.5 A_c\};\ \text{if } N_c > 5.5 A_c \tag{13}$$

where σ_B = cylinder strength of concrete, A_c = the net compression zone area, f_y = yield strength of reinforcement, A_s = the cross-section area of reinforcements, ρ_s = ratio of longitudinal reinforcement, μ = coefficient of friction and N_c = compression force on concrete. Evaluation of shear-friction by Valluvan et al. [6] revealed that if the compression force is greater than $5.5A_c$ (N, mm), the resistance by dowel action of reinforcements will not be effective.

Calculation of shear sliding resistance of steel plates anchored to beam V_s is same as that calculated for shear

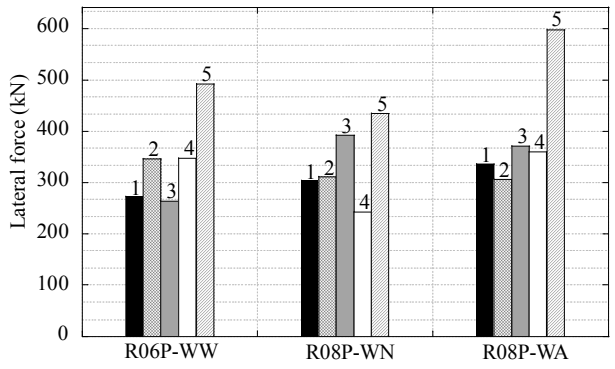

Fig. 8 Calculated lateral strength

resistance by steel plate explained in Part 4.1. The shear resistance by disk-anchor V_{da} was calculated based on the manufacturer's instructions, for example, a disk-anchor system with the characteristics illustrated in Fig. 4 has the lateral shear sliding resistance of V_{da}=80kN at very small displacement (when sliding displacement at potential sliding plane reaches to about 2mm).

4.3 Summary of Calculation

A summary of calculated lateral strengths of the specimens are illustrated at Fig. 8. In specimen **R06P-WW**, diagonal tension crack appeared at the wing-wall-column with high compression force. Since the wing-wall-column was confined by deck steel plates, the lateral resistance did not drop and maintained stable up to drift angle of R=5%. In this specimen, since the compression strut perfectly formed at wing-wall, the compression zone considerably resisted against the shear sliding, and therefore its shear sliding is higher than specimen R08P-WN. It is worthy to note, in calculation of shear strength of wing-wall-column, the contribution of deck plate was not taken into account due to its low in-plane shear resistance. Moreover, in this case, the effectiveness confinement factor was calculated according to Eq. 4 because of low out-of-plane resistance of deck plate. Based on the calculated results, the mechanism 3 (see Fig. 8) is the dominant mechanism.

The specimen **R08P-WN** initially treated as flexural behavior (mechanism 2, see Fig. 8) but after significant yielding of longitudinal reinforcements and deterioration of shear punching resistance, the lateral strength dropped. Then, the lateral strength was governed by shear sliding resistance at top of wing-wall-column with a ductile behavior (mechanism 4).

The specimen **R08P-WA** exhibited a flexural-ductile response by forming perfect plastic hinges at ends of the wing-wall-column (mechanism 2, see Fig. 8). In this specimen when the lateral force acted from left to right, large arch action formed in the right-side wing-wall-column. This specimen can be represented as a well-designed retrofitting scheme for column retrofitted by thick hybrid wing-wall.

5. CONCLUSIONS

(1) In general, application of thick hybrid wing-wall increases lateral strength, stiffness and ductility of the soft-first-story RC frames, as it was obvious through the comparison of experimental results between specimens R07P-P0 and R08P-WA.
(2) The comparison between the results of specimens R06P-WW and R08P-WA, exhibits the influence of jacketing steel plates in shear resistance. Since, in specimen R06P-WW, deck plates were used instead of plain steel plate and deck plates did not have sufficient resistance against out-of-plane deformation, a diagonal tension crack formed in each wing-wall.
(3) The comparison between the governing mechanisms of specimens R08P-WN and R08P-WA, exhibits that the steel plates which were anchored to the top beam had effective contribution in shear-sliding resistance at top of wing-wall.
(4) The retrofit plan of specimen R08P-WA can be considered as well-designed scheme that can obtain the desired seismic performance.
(5) Simplified design equations are suggested for shear strength and shear sliding of wing-wall-columns.

ACKNOWLEDGMENTS

The investigation reported herein was carried out possible by a financial support of the Grant-in-aid for the Science Research (B), (17360272), and (A), (20246091) by Japan Society for the Promotion of Science.

REFERENCES

[1] Rahman, M. N. and Yamakawa, T.: Investigation of Hybrid Technique for Seismic Retrofitting of Bare Frames, Journal of Advanced Concrete Technology, JCI, Vol. 5, No. 2, June, 2007, pp.209-222.
[2] Nielsen, M. P.: Limit Analysis and Concrete in Plasticity, Prentice-Hall, 1984, pp.219-220.
[3] Astaneh-Asl, A.: Seismic Behavior and Design of Steel Shear Walls, Steel TIPS, Structural Steel Educational Council, Moraga, CA, January, 2001.
[4] Yamakawa T., Takara S. & Rahman, M. N.: Cyclic Loading Tests on Retrofitted RC Framed Shear Walls and Their Seismic Performance, Journal of Structural and Construction Engineering, AIJ, Vol. 73, No. 634, Dec., 2008, pp.2167-2174.
[5] ACI Committee 318, Building Code Requirements for Structural Concrete (ACI 318R-05) and Commentary (318R-05), ACI, Farmington Hills, Mich., 2005.
[6] Valluvan, R., Kreger, M. E. and Jirsa, O. J.: Evaluation of ACI 38-95 Shear-friction Provisions, ACI Structural Journal, Proc. V. 96, No. 4, July-Aug., 1999, pp.473-483.